Oxidation of Metals, Vol. 66, Nos. 3/4, October 2006 (© 2006)
DOI: 10.1007/s11085-006-9020-3

Thermal Stability and Oxidation Resistance of Pt–10 Al–4Cr Alloy at Super-High Temperatures

R. N. Mahaptara,* S. K. Varma,†‡ and C. S. Lei*

Received January 26, 2005; revised January 19, 2006

The isothermal-oxidation behavior of refractory superalloy Pt–10Al–4Cr (in at.%) was investigated up to a period of 312 hr in air from 1200 to 1400°C. A comparison of the oxidation behavior of this alloy with a conventional Ni-base superalloy (Inconel 713C) shows an order of magnitude higher oxidation resistance. This experimental alloy oxidizes by forming Al_2O_3 and Cr_2O_3 (and perhaps trace amounts of PtO) with Al_2O_3 as the oxide layer in contact with air. Optical and scanning-electron microscopy (SEM) were used to study the microstructure, morphology, and composition of the scale formed after oxidation. The thermal stability of the alloy after extended periods at 1200, 1300, and 1400°C was studied using transmission-electron microscopy (TEM).

KEY WORDS: oxidation; refractory alloy; weight-gain method; EDS; TEM; SEM; optical microscopy.

INTRODUCTION

The Ni-base superalloys currently used for turbine engines are already operating at up to 90% of their melting temperature. Hence, use of these materials restricts the higher operating temperatures of turbine engines used

*Materials Laboratory, Naval Air System Command, Patuxent River, MD, 20650, USA.
†Department of Metallurgical and Materials Engineering, The University of Texas at, El Paso, El Paso, TX, 79968, USA.
‡To whom correspondence should be sent. e-mail: skvarma@utep.edu

in aviation and power generation. Any further significant improvements in the operating temperatures will require the development of a new class of materials[1] with higher melting points.

One approach is to develop alloys with microstructures analogous to the γ/γ' structures of nickel-base superalloys, but based on elements with higher melting points. In such a microstructure, the FCC matrix is strengthened by coherent precipitates of an intermetallic compound with the Ll_2 (ordered, FCC) crystal structure. The FCC Pt-group metals Pt, Ir and Rh are candidates for such an alloy development program because of their high melting points and exceptional environmental resistance.[2,3]

In a recent study Suss *et al.*[4] explored Pt–Al–Z (Z = Ti, Cr, Ru, Ta, and Re) alloys and reported the effects of various additions on the creep properties of these alloys. The study showed that the Pt–10Al–4Cr alloy has high stress-rupture strength and good room-temperature ductility. However, the details of the oxidation behavior and thermal stability of this alloy have not been evaluated. In this paper, the results of the oxidation behavior and thermal stability of this alloy are reported, and a comparison with Inconel 713C has been made in a temperature range from 1100 to 1400°C.

EXPERIMENTAL PROCEDURES

The Pt–10Al–4Cr alloy was prepared by melting high-purity Pt, Al, and Cr with at least 4 nines purity using a non-consumable electrode arc furnace in a pure–argon gas atmosphere. The as-cast rods were sectioned by electro-discharge machining (EDM) to obtain a nearly cylindrical specimen with 8 mm diameter and 3 mm high. The specimens were polished to a mirror finish in order to remove surface defects. Specimens of about 25.2(1) $\times$ 12.5(w) $\times$ 3.5(t) mm of Inconel 713C were obtained from the General Electric Corporation. These were also polished to a mirror finish before oxidation.

Isothermal-oxidation tests for the Pt–10Al–4Cr alloy were conducted at 1200, 1300, and 1400°C and for Inconel 713C at 1100, 1200, 1300, and 1350°C in air in a top-loading, high-temperature furnace for 312 hr (13 days). Weight-gain measurements of the specimens were performed after every 24 hr.

The microstructure and scale morphology of the oxidized specimens were examined by optical and scanning-electron microscopy (SEM) equipped with high-energy, dispersive spectroscopy (EDS). A JEOL JEM-100CX II transmission-electron microscope (TEM) was used to characterize the microstructural changes taking place during oxidation.

RESULTS AND DISCUSSION

Oxidation Curves

The oxidation curves, weight gain (dW) per unit area (A) vs. exposure time (t), for the experimental alloy and Inconel 713C are shown in Fig. 1. Each curve in this figure represents an average of at least 2 separate experiments at a given temperature. It is obvious that the weight gain per unit area increases with an increase in temperature for both alloys. It should be noted that the oxidation resistance (as indicated by smaller weight gain per unit area) is higher for the alloy compared with the conventional Ni-base superalloy 713C. The oxidation curves shown in this figure were fitted[5] with an empirical equation describing the oxidation kinetics, $dW/A = Kt^n$, where K and n are the constants, and n has been found to be 1/2 for most alloys in the literature. The values of n and the curve-fitting parameter (R^2) can be seen in Table I. It confirms the 1/2 value for n in both alloys at 1200 and 1300°C with the exception at 1350°C for Inconel 713C alloy. It can be an indication of the changes in oxidation mechanisms at different temperatures.

SEM and EDS Results

EDS on the SEM has been used to characterize the oxides formed on the two alloys as shown in Figs. 2 and 3 for the Pt alloy and 713C,

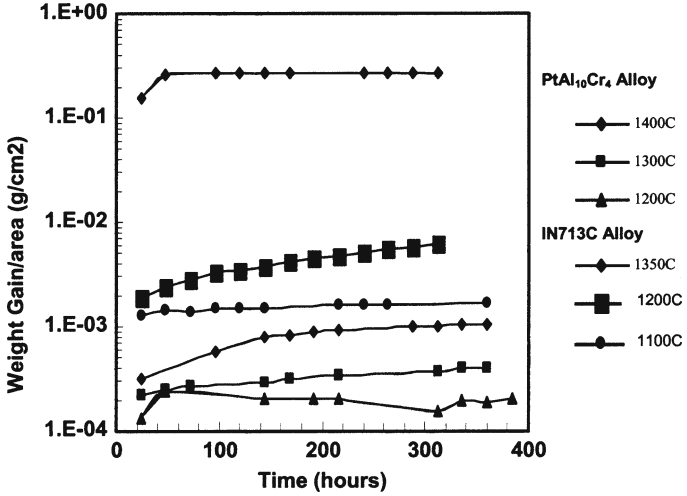

Fig. 1. Oxidation curves for Pt–10A1–4Cr and Inconel 713C alloys over the temperature range of 1200–1400°C.

Table I. Typical Values of n and R for Pt–10Al–Cr and Inconel 713C

Alloy	Temperature (°C)	n	R^2
Pt–10Al–4Cr	1300	0.33	0.99
	1200	0.52	0.98
Inconel 713C	1350	0.16	0.57
	1200	0.46	0.97

respectively. Table II shows the EDS analysis in atomic percents of the scales for the 2 alloys at 1200, 1300 and 1400°C. It must be recalled that the elemental analysis from EDS can be used to identify the most-obvious oxides by taking into account their atomic ratios. Most EDS analyses have such programs incorporated in them. The SEM micrographs in Fig. 2 for Pt–10Al–4Cr indicate the presence of Al_2O_3 as the major constituent, with small amounts (perhaps traces) of Cr_2O_3 and PtO in the oxide scale. Al_2O_3 is present in a dense adherent form at the surface of the scale at all oxidation temperatures (1200, 1300, and 1400°C). The thickness of the scale increases with increasing oxidation temperature. However, a slight decrease in Al_2O_3 and an increase in PtO in the oxide scale were observed in this temperature range of testing when one proceeds from the top of the scale to the interior of the alloy towards the substrate. Figure 3 for Inconel 713C has only dark and light areas corresponding to Al_2O_3 and NiO, respectively. Al_2O_3 is present in a dense form at the surface of the scale at 1200°C, while this trend is reversed (Table III) at 1350°C with more NiO being present in a blocky format at the surface of the specimen instead of Al_2O_3. This is a result of the typical phase stability with respect to the oxidation temperature. A relationship between the oxidation curves, SEM micrographs, and the results of EDS analysis leads us to believe that Al_2O_3 is the protective layer while NiO, perhaps, lowers the oxidation resistance.

Temperature Dependence

The temperature dependence of the oxidation kinetics is expressed by an Arrhenius type: $K = K_0.\exp(-Q/RT)$, where K_0 is a temperature-independent constant, R is the universal gas constant, and Q is the activation energy for oxidation. Figure 4 shows the variation of K with the reciprocal of absolute temperature on a semi-log plot. The plot includes only 2 data points since the parabolic fit to the oxidation curves do not allow the calculation for activation-energy values, Q, with similar oxidation mechanisms. In fact the oxidation curve at 1400°C can be fitted better with a linear

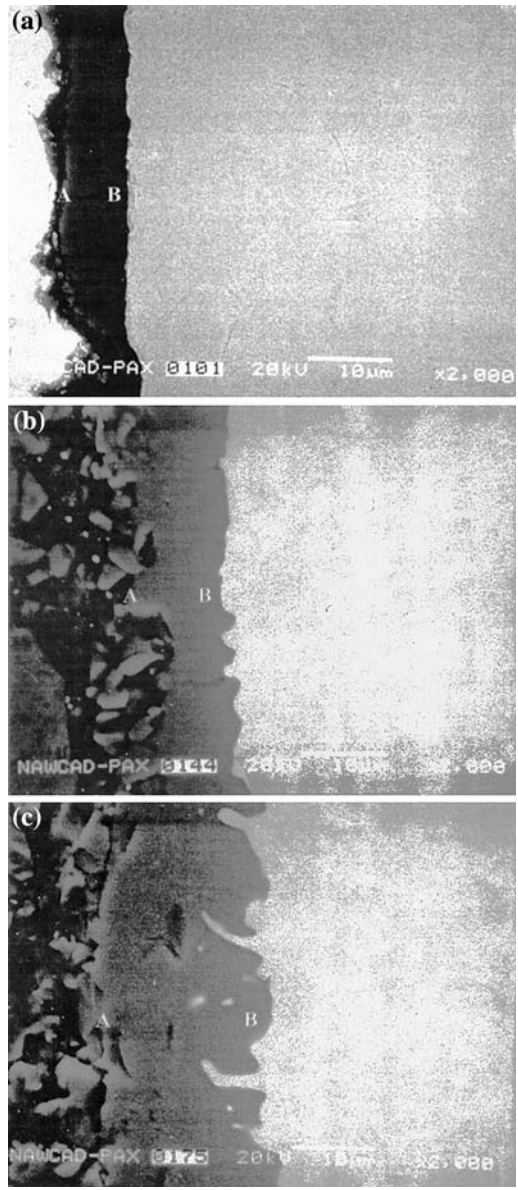

Fig. 2. SEM micrographs showing the nature of scales formed at (a) 1200, (b) 1300, and (c) 1400°C for Pt–l0Al–4Cr. Table II shows the EDS results at points marked in the SEM micrographs.

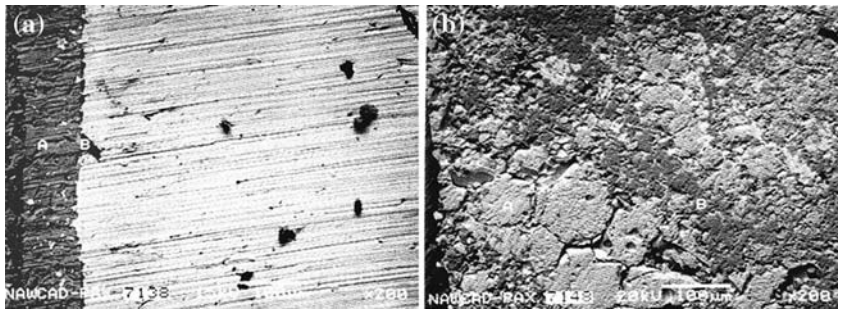

Fig. 3. SEM micrographs showing the nature of scales formed at (a) 1200, and (b) 1350°C for Inconel 713C. Table III shows EDS results at points marked in the SEM micographs.

Table II. EDS Analysis of the Scales on Pt–40AI–4Cr at 1200, 1300 and 1400°C (in at%)

Temperature (°C)	A	B
Pt–10Al–4Cr		
1200°C		
Al_2O_3	98.08	24.91
Cr_2O_3	1.47	1.88
PtO	0.45	73.21
1300°C		
Al_2O_3	98.75	12.70
Cr_2O_3	0.73	1.89
PtO	0.52	85.40
1400°C		
Al_2O_3	98.28	17.80
Cr_2O_3	0.97	0.70
PtO	0.75	81.50

Table III. EDS Analysis of Scales on Inconel 713C at 1200 and 1350°C (in at.%)

Temperature (°C)	A	B
Inconel 713C		
1200°C		
Al_2O_3	97.06	89.63
NiO	1.67	5.61
TiO_2	0.10	3.39
1350°C		
Al_2O_3	4.27	22.55
NiO	91.72	54.50
TiO_2	0.53	2.15

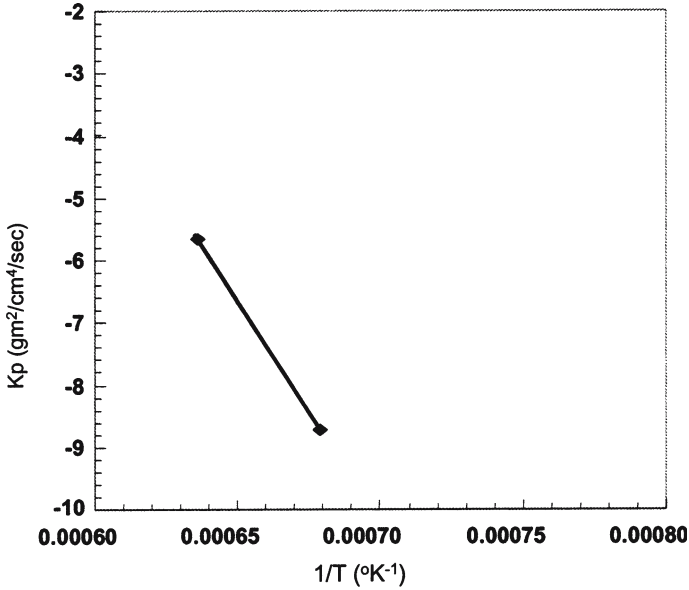

Fig. 4 Arrhenius plot for Pt–10A–4Cr using the data showing parabolic oxidation curves in Fig. 1.

relationship between weight gain per unit area and oxidation time. The calculated Q from the slope of the line in this figure has been found to be 14 kcal/mol for the Pt–10Al–Cr alloy as shown in Table IV.

The relatively high Q values for the Pt alloy[6,7] of this study can be considered as an indication for higher oxidation resistance based on the assumption that Q represents the activation energy for oxidation[6,7] and similar oxidation mechanisms are operative in the temperature range of this study. The high activation energy for oxidation of the alloy may be attributed to the formation of Al_2O_3 in the scale.

Table IV. Activation-energy Values for Pt–10Al–4Cr, Inconel 713C, and Ti–44Al-xNb Alloys

Alloy	Q(kcal/mole)	Reference
Pt–10Al–4Cr	141.0	This study
Inconel 713C	104.3	Mahapatra *et al.*[6]
Ti-44Al-xNb	56–100	Woo *et al.*[7]

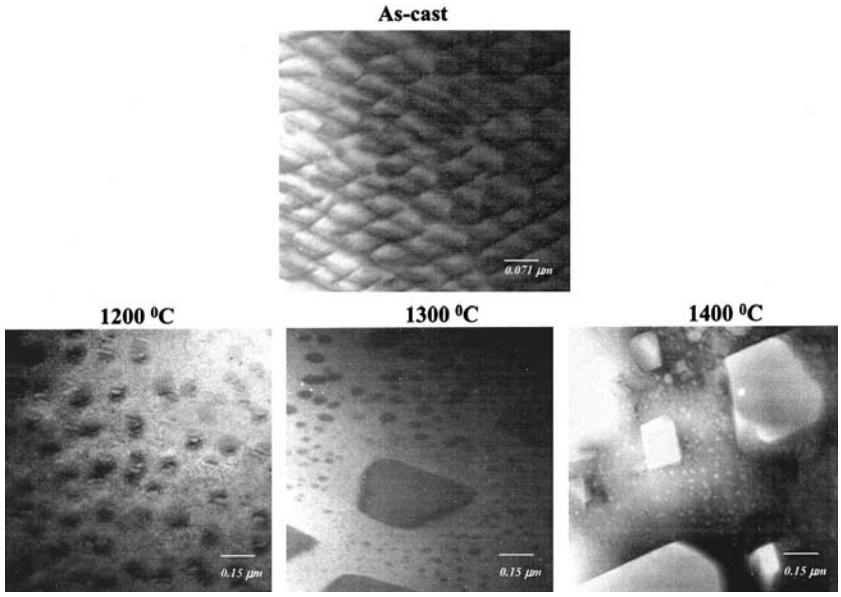

Fig. 5 TEM of Pt–10A1–4Cr in as-cast and heat-treated condition at 1200, 1300, and 1400°C for 312 hr in air. It shows a morphological change of the second-phase from a basket-weave morphology in the as-cast condition to an orthogonal/round shape precipitates after oxidation.

Thermal Stability

Figure 5 shows a comparison of the microstructures for the Pt–10Al–4Cr alloy exposed at 1200, 1300, and 1400°C in air for 312 hr along with the as-cast structure. These temperatures were selected in order to determine the phase stability in this alloy at high temperatures for potential advanced propulsion systems to replace currently used Ni-base alloys, The breakdown of the basket-weave type of second phase distribution to nearly orthogonal/round shaped particles at high temperature exposure is clearly an indication that the second phase is trying to reduce its total surface energy through the process of shpheroidization. The growth of precipitates appears to be stable up to 1300°C but excessive growth is taking place at temperatures above this. Thus thermal stability of the alloy at temperatures above 1300°C can be questioned.

CONCLUSIONS

1. Pt–10Al–4Cr alloy has an order-of-magnitude higher oxidation resistance compared to the Ni-base superalloy, Inconel 713C, at 1200, 1300, and 1400°C in air up to 312 hr.

2. Pt–10Al–4Cr forms an adherent Al_2O_3 protective oxide when exposed to air at 1200, 1300, and 1400°C for 312 hr.
3. The thermal stability shows that the basket-weave, second-phase structure in the as-cast condition breaks down to a pseudo-spheroidized structure when exposed at 1200, 1300, and 1400°C in air for 312 hr.

REFERENCES

1. C. T. Sims, N. S. Stoloff, and W. C. Hagel, *in Superalloy II: High Temperature Materials For Aerospace and Industrial Power* (USA: Wiley-Interscience, 1987).
2. Y. Yamabe-Mitarai, Y. Koizumi, H. Murakami, Y. Ro, T. Maruko, and H. Harada, *Scripta Materialia* **35**, 211 (1996).
3. Y. Yamabe-Mitarai, Y. Ro, T. Maruko, T. Yokokawa, and H. Harada, *Structural Intermetallics* 805 (1997).
4. R. Suss, D. Freund, R. Volkl, B. Fischer, P. J. Hill, P. Ellis, and I. M. Wolff, *Materials Science and Engineering A* **338**, 133 (2002).
5. M. G. Montana, and N. D. Greene, *in Corrosion Enineering, Materails Science and Engineering Series* (New York: McGraw-Hill, 1978), pp. 347.
6. R. N. Mahapatra, S. K. Varma, C. Lei, and V. V. Agarwala, *Oxidation of Metals* **62**(1/2), 93 (2004).
7. J. W. Woo, S. K. Varma, and R. N. Mahapatra, *Metallurgical and Materials Transactions A* **34**, 2263 (2003).